Diurnal Self-Aggregation

— Supplementary Information —

Jan O. Haerter, Bettina Meyer, Silas Boye Nissen

In this supplementary information, we provide further analysis of interest to expert readers, but not needed for the understanding of the main text.

Note on Supplementary Figure 6: Convective Available Potential Energy (CAPE) is defined column-wise as $CAPE \equiv g \int_{LFC}^{LNB} dz\ \theta_v'$ with $g = 9.81\,m\ s^{-2}$ the gravitational acceleration, LFC and LNB the levels of free convection and neutral buoyancy, respectively, and $\theta_v' \equiv (\theta_{v,p}(z) - \theta_{v,e}(z))/\theta_{v,e}(z)$ the virtual potential temperature, where $\theta_{v,e}(z)$ and $\theta_{v,p}(z)$ are the respective virtual potential temperatures of the environment at height z and a parcel that is lifted from the lowest model level to height z.

To test how different fields co-vary, we make use of the Pearson correlation function between any two fields v and w, which is defined as $cov(v,w) \equiv \overline{v' \cdot w'}/(\sigma(v)\sigma(w))$, with the overbar denoting the horizontal domain mean, $\sigma(v)$ the standard deviation of v and $v' \equiv v - \overline{v}$ the deviation from the horizontal domain mean. Note that $cov(v,w) \in [-1,1]$ normalises to the standard deviations of the two fields, hence, even fields with small overall fluctuations can show large Pearson correlations.

To understand precursors of precipitation, we consider co-variation of rain intensity I, averaged over the first two hours after the onset, with CAPE and cloud-base moisture at rain onset time. Rain onset time (04:00 for $A2$, and 09:40 for $A5$) is defined as the time when domain mean precipitation exceeds $0.02\,mm\,s^{-1}$, a threshold chosen to neglect nocturnal precipitation in $A2$ but capture the pronounced daytime peak. Both CAPE and cloud-base moisture show significant correlation with precipitation intensity. CAPE and rain intensity, I, co-vary for $A5$, with $cov(CAPE, I) \approx .1$, significantly exceeding $cov(CAPE, I) \approx .01$ for spatially randomised CAPE or $cov(CAPE, I) \approx .03$ for $A2$. Similarly, precipitation is enhanced in areas of positive cloud-base moisture anomaly (defined as $q_{v,mid} \equiv \int_{500m}^{2200m} q_v(z)dz$), with $cov(q_{v,mid}, I) \approx 0.4$ for both $A2$ and $A5$.

We find CAPE to be enhanced in regions with positive near-surface specific humidity anomalies $q_{v,srf}$ (defined here as $q_{v,srf} \equiv \int_{0m}^{300m} q_v(z)dz$, where the integral is numerically discretised according to vertical model levels), with a relatively strong signal, $cov(CAPE, q_{v,srf}) \approx .7$, both for $A5$ and $A2$. Near-surface specific humidity in turn is correlated with cloud-base specific humidity $q_{v,mid}$, with $cov(q_{v,sfc}, q_{v,mid}) \approx .3$ and $\approx .4$ for $A2$ and $A5$, respectively, indicating an enhanced correlation of cloud-base moisture with CAPE for $A5$, with $cov(CAPE, q_{v,mid}) \approx 0.2$, and $\approx .3$ for $A2$ and $A5$, respectively.

Thus, for $A5$, CAPE, $q_{v,srf}$ and $q_{v,mid}$ act as precursors for enhanced surface rain intensity I.

Experiment Name	Mean Event Density N/A $[km^{-2}]$	Mean Event Intensity $\langle I_e \rangle$ $[mm\ h^{-1}]$	Mean Event Area a_0 $[km^2]$	Mean Track Duration D $[min]$
A5a	.016	4.6	22.4	61
A2a	.013	4.7	19.8	76
A5b	.019	4.5	22.0	55
A2b	.016	4.75	19.3	65
A5c	.027	4.73	16.1	45
A5d	.12	4.98	19.2	48
A3.5	.017	4.41	19.2	62
A5sea	.016	5.32	30.0	65
A2sea	.021	4.96	20.1	75
A5vent05	.021	4.27	16.6	62
A5vent001	.026	4.05	13.8	63
A5p2K	.016	4.94	28.4	55
A5ph3.6	.011	4.44	27.6	66
A5ph6	.012	4.44	27.5	65
A0	.016	4.96	20.0	66
A5constrad	.011	4.47	27.5	65
A0constrad	.009	5.03	27.4	70

Supplementary Table 1: **Basic statistics for all numerical experiments.** The table lists basic statistics as a general overview of the events and tracks in each experiment. Mean values were computed for all available days except days one and two, which were considered transient. The main four experiments are listed above the horizontal line (A5a, A2a, A5b, A2b). Sensitivity experiments are listed below the horizontal line. Note that some caution should be exercised in interpreting means for experiments with only a single day of data.

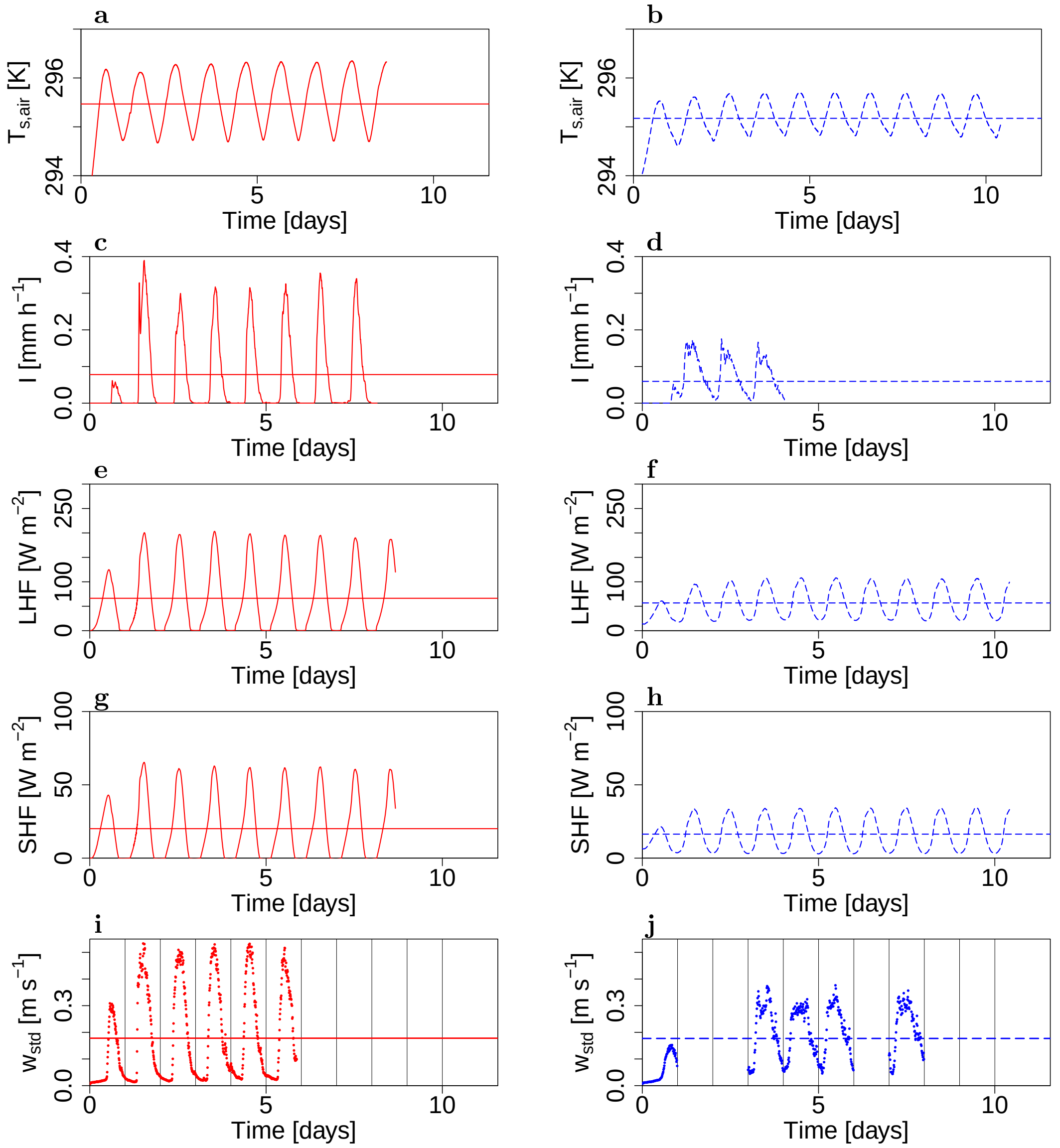

Supplementary Figure 1: **Multi-day time series of domain averaged quantities**. **a**, Domain-mean near-surface temperature ($T(z = 50\ m)$) for the simulation A5b. The horizontal line indicates the time average over the entire time series; **b**, Analogous to (a), but for *A2b* (*compare*: Tab. 1); data beyond day four in (d) were discarded; **c,d**, Analogous to (a),(b), but for domain mean precipitation intensity; **e,f**, Analogous to (a),(b), but for the surface latent heat flux; **g,h**, Analogous to (a),(b), but for the surface sensible heat flux. **i**, the standard deviation of horizontal fluctuations in vertical velocity at $z = 1\ km$ for *A5a*; **j**, similar to (i) but for *A2a*. Note that nocturnal w_{std} is extremely small, and in particular much smaller for *A5b* than for *A2b*. This implies that any memory harboured by circulation should be negligible for *A5b* in comparison to *A2b*.

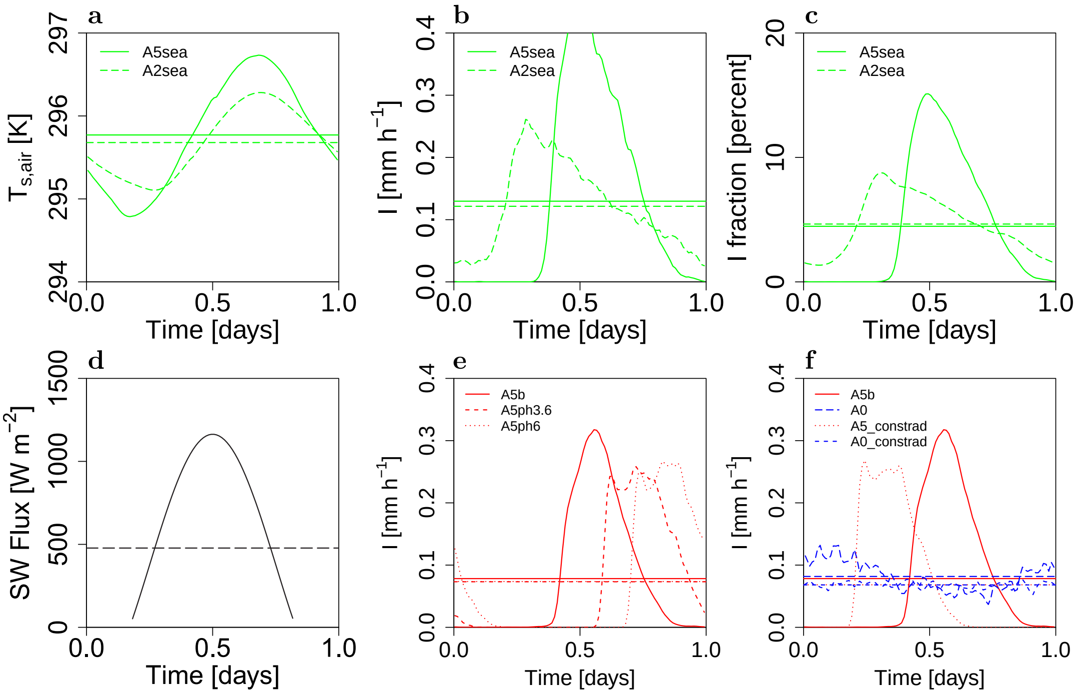

Supplementary Figure 2: **Diurnal cycles of domain averaged quantities**. **a**—**c**, Similar to Fig. 1 but for a sea surface (*A2sea* and *A5sea*, respectively, *compare*: Tab. 1). **d**, Shortwave downwelling flux, that is, the solar radiative flux, at the top of the atmosphere, showing the case of variable flux (solid curve) and constant flux (dashed). **e**, Sensitivity to a phase shift of surface temperature by $\tau = 3.6$ h and $\tau = 6$ h, respectively (*compare* Tab. 1 and Eq. 6). **f**, Sensitivity to constant solar radiation and/or constant surface temperature (*compare* Tab. 1).

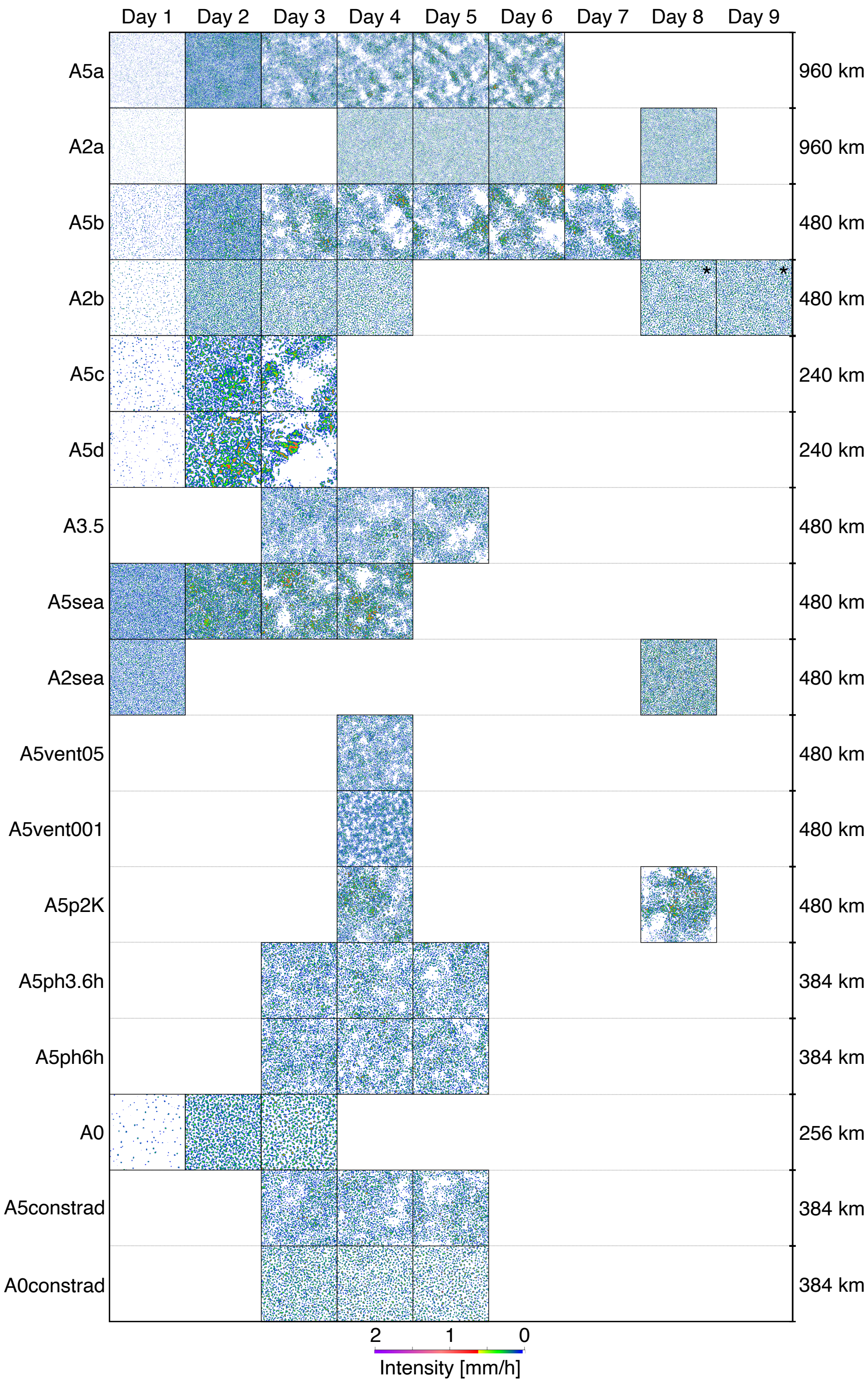

Supplementary Figure 3: **Daily average precipitation intensity for all available data.** Similar to the heatmaps shown in Fig. 1. The asterisks (*) indicate simulation A2long (*compare*: Tab. 1).

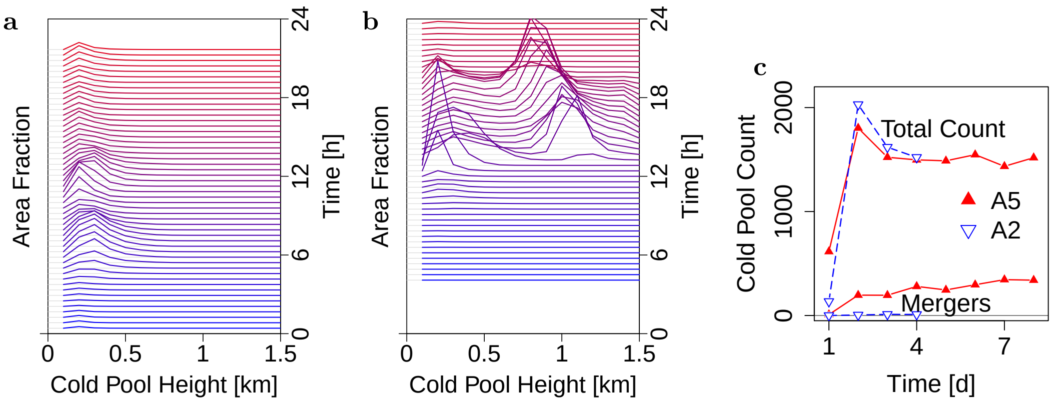

Supplementary Figure 4: **Cold pool height distribution functions.** **a**, Cold pool height distribution function for day four of A2b (*compare*: Fig. 3b). Each curve shows the histogram for all cold pool heights within five model timesteps (right vertical axis), that is, $480 \times 480 \times 5$ individual height values. A dominant peak occurs at the surface, which is not shown, as it corresponds to regions without cold pools. This explains why some curves show a larger probability weight than others. The probability origin of each curve is shifted and marked by a grey horizontal line. Colours from blue to red indicate increasing time, as indicated along the y-axis on the right. **b**, Analogous to (a), but for A5b during day four (*compare*: Fig. 3d). Note the pronounced double-peak structure that emerges for A5b near mid-day. **c**, Statistics of the number of CPs and mergers as a function of time, for *A5b* and *A2b*. Note that mergers are much more frequent for *A5b*, whereas the total count of CPs is similar for the two simulations.

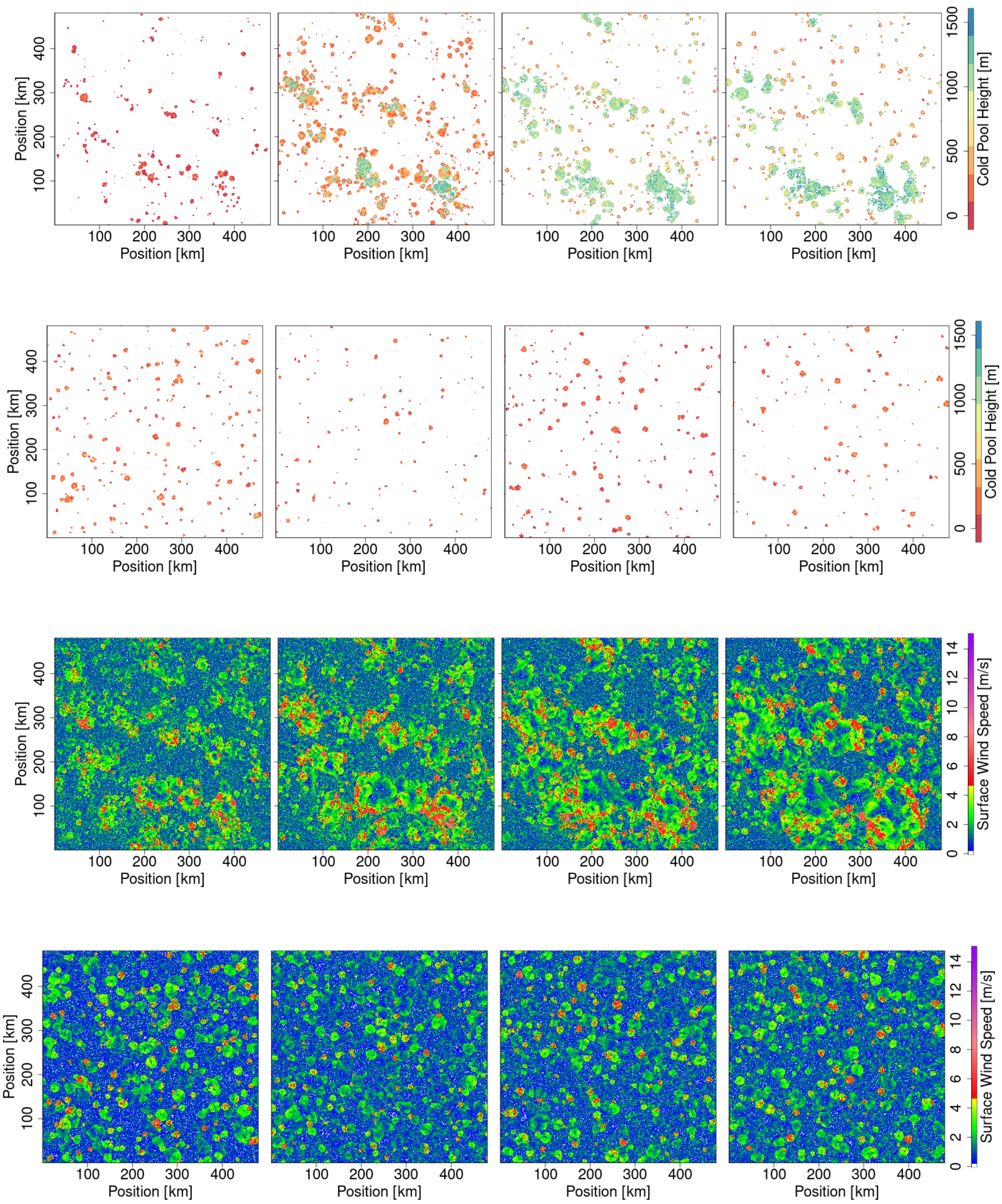

Supplementary Figure 5: **Cold pool height and near surface horizontal wind speed.** *Top row*, CP heights for A5b, day 4, at times $t = \{12.5, 13.5, 14.5, 15.5\}$ hours. *Second row*, CP heights for A2b, day 4, at times $t = \{7, 9, 11, 13\}$ hours. (*compare*: Fig. 4). *Third row*, surface wind speed for A5b, day 4, at times $t = \{12.5, 13.5, 14.5, 15.5\}$ hours. *Bottom row*, surface wind speed for A2b, day 4, at times $t = \{7, 9, 11, 13\}$ hours.

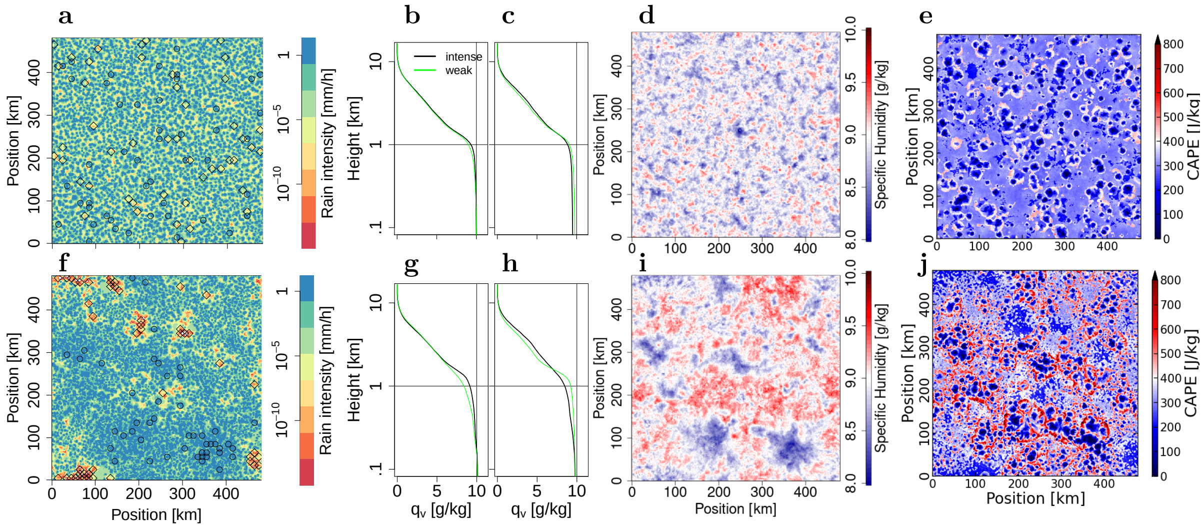

Supplementary Figure 6: **Moisture oscillations.** **a**, Simulation *A2b* on day four. Spatial rain distribution (red) with extreme rainfall highlighted (top and lowest two percent, that is intense and weak values, marked in circles and diamonds, respectively). **b**, Vertical specific humidity profile, $q_v(z)$, before the onset of precipitation in *A2b* (at 2 h local time) for sub-regions of intense (top two percent) and weak (lowest two percent) daily-averaged rain rate; horizontal and vertical thin black lines are a guide to the eye. **c**, Analogous to (b), but at the end of the model day (at 22h local time). **d**, Daily-mean specific humidity at $z = 1050\,m$ for *A2b* on day four. **e**, CAPE at peak time of precipitation (06:50 h local time) for *A2b* on day four. (*See* the note at the beginning of the Supplementary Information on how we define CAPE). **f—j**, Analogous to (a)—(e), but for *A5b* (vertical profiles at 5 h and 22 h local time, respectively, rainfall peak at 13:25 h; rain onset at 9 h); Increased $cov(CAPE, q_{v,mid})$ and $cov(CAPE, I)$ for A5 indicate CAPE as a precursor of convection (*Details:* SI Text). Note the logarithmic vertical axis scaling in panels b,c,g,h.

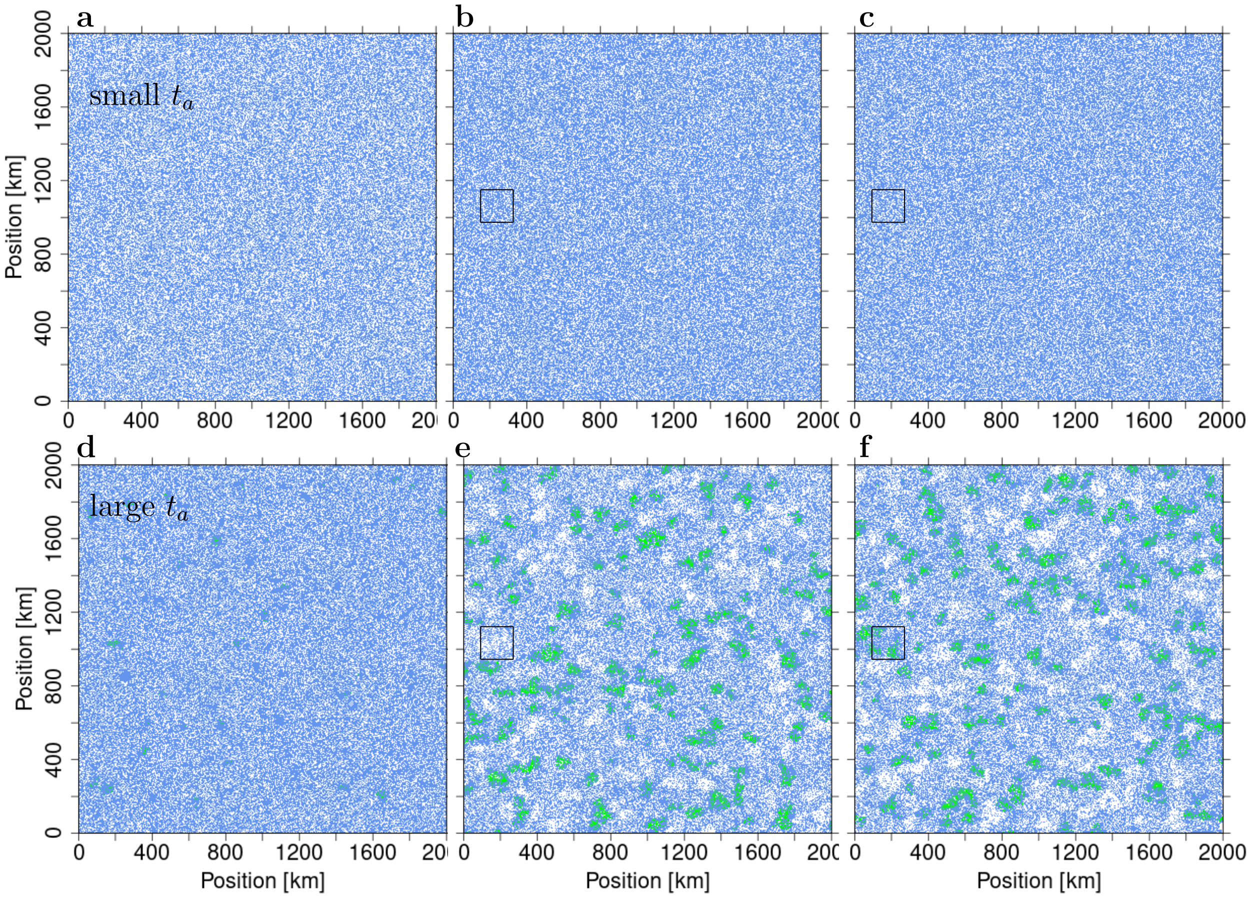

Supplementary Figure 7: **Transition to a clustered rainfall state in the simplified model.** **a**, Surface rainfall average during the first day ($t = 1\ d$, spin-up) for $\Delta T = 2\ K$. **b**, Similar to (a), but for $t = 6\ d$. **c**, Similar to (a), but for $t = 7\ d$. **d**—**f**, Similar to (a)—(c), but for a large diurnal surface temperature amplitude. To highlight the spatial and temporal variation, boxes of side length $l = 180\ km$ are shown at equal positions in panels b,c,e,f. Pixels in white, blue and green correspond to zero, one, or two rain events, occurring within the particular model day.